Large Molecule Therapeutics

Molecular Cancer Therapeutics

Preclinical Evaluation of Multistep Targeting of Diasialoganglioside GD2 Using an IgG-scFv Bispecific Antibody with High Affinity for GD2 and DOTA Metal Complex

Sarah M. Cheal[1], Hong Xu[2], Hong-fen Guo[2], Pat B. Zanzonico[3], Steven M. Larson[3,4], and Nai-Kong Cheung[2,4]

Abstract

Bispecific antibodies (BsAb) have proven to be useful targeting vectors for pretargeted radioimmunotherapy (PRIT). We sought to overcome key PRIT limitations such as high renal radiation exposure and immunogenicity (e.g., of streptavidin–antibody fusions), to advance clinical translation of this PRIT strategy for diasialoganglioside GD2-positive [GD2(+)] tumors. For this purpose, an IgG-scFv BsAb was engineered using the sequences for the anti-GD2 humanized monoclonal antibody hu3F8 and C825, a murine scFv antibody with high affinity for the chelator 1,4,7,10-tetraazacyclododecane-1,4,7,10-tetraacetic acid (DOTA) complexed with β-particle–emitting radiometals such as ^{177}Lu and ^{90}Y. A three-step regimen, including hu3F8-C825, a dextran-based clearing agent, and *p*-aminobenzyl-DOTA radiolabeled with ^{177}Lu (as ^{177}Lu-DOTA-Bn; $t_{1/2} = 6.71$ days), was optimized in immunocompromised mice carrying subcutaneous human GD2(+) neuroblastoma (NB) xenografts. Absorbed doses for tumor and normal tissues were approximately 85 cGy/MBq and ≤3.7 cGy/MBq, respectively, with therapeutic indices (TI) of 142 for blood and 23 for kidney. A therapy study ($n = 5$/group; tumor volume, 240 ± 160 mm^3) with three successive PRIT cycles (total ^{177}Lu: ∼33 MBq; tumor dose ∼3,400 cGy), revealed complete tumor response in 5 of 5 animals, with no recurrence up to 28 days after treatment. Tumor ablation was confirmed histologically in 4 of 5 mice, and normal organs showed minimal overall toxicities. All nontreated mice required sacrifice within 12 days (>1.0-cm^3 tumor volume). We conclude that this novel anti-GD2 PRIT approach has sufficient TI to successfully ablate subcutaneous GD2(+)-NB in mice while sparing kidney and bone marrow. *Mol Cancer Ther; 13(7); 1803–12. ©2014 AACR.*

Introduction

Pretargeted radioimmunotherapy (PRIT) offers the promise of greatly improved therapeutic indices (TI) for delivery of internal radiation to solid human tumors, including diasialoganglioside GD2-positive neuroblastoma [GD2(+)-NB]. Successful PRIT of GD2(+)-NB has been demonstrated using streptavidin–antibody fusion constructs, owing to its high antigen density (5×10^6 molecules per NB cell) and the slow internalization rate of the anti-GD2 antibody/GD2 complex from the NB cell surface. A typical PRIT protocol begins with a cold dose of bispecific antibody (BsAb) to prelocalize at the tumor, followed with a clearing agent (CA) to remove circulating off-target antibody and then last, a rapidly clearing radiolabeled small-molecule hapten or peptide.

Previously, we developed an anti-GD2 single-chain antibody–streptavidin fusion protein [5F11-scFv-SA (streptavidin)] for delivery of radiolabeled biotin, observing tumor-to-blood radiation dose ratios as high as 160:1 in mouse models of human GD2(+)-NB (1). During parallel therapy studies with radioiodinated anti-GD2 monoclonal antibody (mAb) 3F8 (^{131}I-3F8), a tumor-to-blood ratio of 2.7:1 was achieved, demonstrating the dosimetric advantage of PRIT over conventional radioimmunotherapy (i.e., with directly labeled antibodies or antibody fragments). Despite this, additional optimization of PRIT with 5F11-scFv-SA is required to address the high immunogenicity of streptavidin and high kidney exposure due to prolonged retention of 5F11-scFv-SA in the renal cortex.

As an alternative to streptavidin/biotin, other high-affinity antibody–hapten pairs have been developed for PRIT (2). Over two decades ago, Reardan and colleagues pioneered a PRIT system using antibodies against metal chelates (3). The mAb 2D12.5 has nmol/L affinity for low molecular weight (MW) 1,4,7,10-tetraazacyclododecane-1,4,7,10-tetraacetic acid (DOTA) complexes with yttrium (Y) and lutetium (Lu), and is well suited for PRIT *in vivo*

Authors' Affiliations: Departments of [1]Radiology and [2]Pediatrics; [3]Molecular Pharmacology and Therapy Service; and [4]Program in Molecular Pharmacology and Chemistry, Memorial Sloan Kettering Cancer Center, New York, New York

Note: Supplementary data for this article are available at Molecular Cancer Therapeutics Online (http://mct.aacrjournals.org/).

Corresponding Author: Nai-Kong V. Cheung, Department of Pediatrics, Memorial Sloan Kettering Cancer Center, 1275 York Avenue, New York, NY 10065. Phone: 646-888-2313; Fax: 646-422-0452; E-mail: cheungn@mskcc.org

doi: 10.1158/1535-7163.MCT-13-0933

(4). Orcutt and colleagues subsequently affinity matured the 2D12.5 sequence to yield a novel scFv ("C825") with pmol/L affinity with improved dissociation half-time of the antibody–DOTA complex (from 5.5 minutes to ~5 hours; ref. 5). Specifically intended for PRIT, multiple IgG-scFv BsAb were developed consisting of an IgG with specificity to a cancer cell surface target [e.g., carcinoembryonic antigen (CEA) or A33] linked to C825 scFv at the C-terminus of the IgG light chains as an IgG-scFv format (6). The IgG-scFv BsAbs were sufficiently functional and stable *in vivo* to permit highly efficient tumor targeting of the ^{177}Lu-DOTA hapten in mouse xenograft models of human adenocarcinoma (e.g., tumor-to-tissue uptake ratios of >450 for blood and >20 for kidneys; ref. 7). On the basis of these reports, as well as our aforementioned experience pretargeting GD2(+)-NB, we reasoned that anti–GD2-C825 could offer a viable clinical developmental path for PRIT directed at GD2(+)-NB.

In this report, we describe the initial demonstration of hu3F8-C825 for PRIT of GD2(+)-NB. The novel BsAb was prepared by cloning and expression of the sequences for hu3F8 (8) and C825 as an IgG-scFv format, followed with purification, and extensive biochemical and functional characterization *in vitro*. Next, the BsAb was radiolabeled with the positron-emitting isotope ^{124}I ($t_{1/2}$ = 4.18 days; ^{124}I-hu3F8-C825) for noninvasive serial positron emission tomography (PET) of GD2(+) tumor targeting and plasma clearance, followed with sacrifice of each animal for harvesting of select tissues for assay of radioactivity uptake and biodistribution. For PRIT of GD2(+)-NB with hu3F8-C825, a three-step strategy was developed consisting of injections of hu3F8-C825, a dextran-based CA, and ^{177}Lu-DOTA-Bn hapten. Although C825 scFv has affinities in the range of approximately 15 pmol/L for each Lu- and Y-DOTA-Bn (5), ^{177}Lu was used for this approach primarily because of its theranostic radionuclide properties (β-maximum energy, 0.5 MeV; β-average energy, 0.13 MeV; γ, 208 keV, 11% abundance), as well as reports suggesting that PRIT with ^{177}Lu may result in lower off-target doses compared with ^{90}Y and ^{131}I (9). Finally, additional PRIT experiments were performed to estimate the radiation exposure to various tissues and to predict dose-limiting organ toxicity, followed with a pilot therapy study to evaluate therapeutic efficacy and overall toxicity.

Materials and Methods

Tumor cell lines and cell culture reagents

The human GD2(+)-NB IMR-32, as well as the GD2-negative [GD2(−)] cell lines SK-N-SH (NB) and BT474 (human breast cancer in which GD2 is present on a small subset of stem cells; ref. 10) were obtained from the American Type Culture Collection and maintained pursuant to the manufacturer's recommendations. The luciferase-labeled GD2(+)-NB tumor cell line IMR-32-Luc was generated by stably expressing an SFG-GFLuc vector into the IMR-32 cells (11). All cell lines were initially cultured and cryopreserved in small aliquots to limit passages to less than 3 months, and periodically tested for mycoplasma using a commercial kit (Lonza). IMR-32, IMR-32-Luc, and SK-N-SH culture media were supplemented with 10% FBS and 100 U/mL of each penicillin and streptomycin. BT474 culture media were supplemented with nonessential amino acids, 10% FBS, and 100 U/mL of each penicillin and streptomycin.

Cloning and expression of hu3F8-C825

The BsAb format was designed similar to that described by Orcutt and colleagues, as a C825–scFv fusion to the C-terminus of the light chain of a human IgG (6). The heavy chain is the same as that of human IgG1 except N297A mutation for aglycosylated form, whereas the light chain is constructed as leader VL-Cκ-$(Gly_4Ser)_2$-scFv. Nucleotide sequences encoding VH and VL domains from our hu3F8, and the disulfide-stabilized C825 scFv were synthesized by GenScript with appropriate flanking restriction enzyme sites, and were subcloned into our standard mammalian expression vector.

Linearized plasmid DNA was used to transfect CHO-S cells (Invitrogen) for stable production of BsAb. One million cells were transfected with 2.5 μg of plasmid DNA by Nucleofection (Lonza) and then recovered in CD OptiCHO medium supplemented with 8 mmol/L L-glutamine (Invitrogen) for 2 days at 37°C in 6-well culture plates. Stable pools were selected first with 500 μg/mL hygromycin for approximately 2 weeks and single clones were then selected out with limited dilution. BsAb titer was determined by GD2 and BSA-(Y)-DOTA-Bn ELISA, respectively. Two million cells from several high-expression clones were grown in 10 mL media per T25 flask for 4 days, and supernatants were harvested for further analysis and selection of the optimum clone.

The BsAb producer line was cultured in OptiCHO medium and the mature supernatant harvested. A protein A affinity column (GE Healthcare) was preequilibrated with 25 mmol/L sodium citrate buffer with 0.15 mol/L NaCl, pH 8.2, and bound BsAb was eluted with 0.1 mol/L citric acid/sodium citrate buffer, pH 3.9, and alkalinized (1:10 *v*/*v* ratio) in 25 mmol/L sodium citrate, pH 8.5. The total yield of BsAb was 5 to 10 mg/L. For storage, BsAb was dialyzed into 25 mmol/L sodium citrate, 0.15 mol/L NaCl, pH 8.2, and frozen in aliquots at −80°C.

Surface plasmon resonance studies

Biacore T-100 Biosensor, CM5 sensor chip, and related reagents were purchased from GE Healthcare. The gangliosides GM1 was from ALEXIS Biochemicals (AXXORA L.L.C.) and GD2 from Advanced ImmunoChemical. A BSA-(Y)-DOTA-Bn conjugate was prepared by reacting the *p*-isothiocyanate–DOTA-(Y) complex (prepared according to Corneillie and colleagues; ref. 12) with the albumin using protocols described in Hermanson (13). Gangliosides were directly immobilized onto the CM5 sensor chip (GD2 and GM1 in a 1:1 ratio for the active surface, and GM1 only for the reference) via hydrophobic interaction (14). Separately, BSA-(Y)-DOTA-Bn (active surface) and BSA (reference surface) were immobilized

using the Amino Coupling Kit (GE Healthcare). Purified BsAbs and control antibodies (hu3F8; ref. 8) for GD2 and A33-C825 (6) for BSA-(Y)-DOTA-Bn) were analyzed, and data were fit to a 1:1 binding model (for GD2) or bivalent analyte model (for BSA-(Y)-DOTA-Bn) using the Biacore T-100 evaluation software.

Radiolabeling of hu3F8-C825 and DOTA-Bn hapten

^{124}I was either provided in-house by the Memorial Sloan Kettering Radiochemistry and Molecular Imaging Probes Core Facility or purchased commercially (IBA Molecular). Stocks of hu3F8-C825 were labeled with radioactive iodine using precoated IODOGEN tubes (Pierce) according to standard protocols (15, 16) to final specific activities of 121 to 152 MBq/mg. The tracer immunoreactivities were evaluated using cell-binding assays (17) and were 78.8% ± 0.1% ($n = 3$) for GD2(+)-NB IMR-32 and 4.9% ± 0.4% ($n = 3$) for GD2(−) SK-N-SH. The chelate *p*-aminobenzyl–DOTA (DOTA-Bn; Macrocyclics) was radiolabeled with $^{177}LuCl_3$ (specific activity: 170 MBq/(nmoles); PerkinElmer) at a ratio of 37 MBq to 1.1 μmoles DOTA-Bn using previously described methods (9), but without HPLC purification (C825 does not recognize metal-free DOTA-Bn).

Xenograft studies

All animal experiments were approved by the Institutional Animal Care and Use Committee of Memorial Sloan Kettering Cancer Center (New York, NY), and institutional guidelines for the proper and humane use of animals in research were followed. Athymic nu/nu female mice (6–8 weeks old; Harlan Sprague Dawley) were allowed to acclimate in the vivarium for at least 1 week. For the BT474 tumor model, mice were implanted with estrogen (17β-estradiol; 0.72 mg/pellet 60-day release; Innovative Research of America) by Trochar 3 days before inoculation with cells. Groups of animals were injected subcutaneously with either IMR-32-Luc or BT474 in the left flank with 5×10^6 cells formulated 1:1 with Matrigel (BD Biosciences), and tumors were observed in 3 to 6 weeks (volume, V: 200–500 mm^3 for IMR-32-Luc and 150–300 mm^3 for BT474 using the formula for the volume of an ellipsoid $V = 4/3\pi(length/2 \times width/2 \times height/2$; ref. 18). All reagents were given intravenously via the lateral tail vein. The PRIT protocol included injection of hu3F8-C825 ($t = -28$ hours), followed 24 hours later by CA or vehicle [the CA is a 500 kDa dextran-(Y)-DOTA-Bn conjugate, prepared according to Orcutt and colleagues; ref. 7); the substitution ratio of (Y)-DOTA-Bn (in moles) per mole of dextran ranged from 61 to 161 (Y)-DOTA-Bn/dextran; $t = -4$ hours)], and ^{177}Lu-DOTA-Bn (5.6 MBq, 33 pmoles) after 4 hours ($t = 0$ h). The timing between injection of hu3F8-C825 and CA was based on the PET imaging studies with ^{124}I-hu3F8-C825, whereas a time interval of 4 hours was initially chosen for the CA and ^{177}Lu-DOTA-Bn. For *ex vivo* biodistribution analysis, mice were euthanized, and tumor and selected organs were harvested, weighed, and radioassayed by gamma scintillation counting (Wallac Wizard 3 automatic gamma counter, PerkinElmer). Count rates were converted to activities using a system calibration factor, decay corrected and normalized to the administered activity, and expressed as the percentage of injected dose per gram (%ID/g).

PET and scintigraphy imaging studies

IMR-32-Luc GD2(+)-NB tumor-bearing mice ($n = 5$) were injected intravenously with 8.5 to 10.2 MBq of ^{124}I-hu3F8-C825 (280–500 pmoles) and placed under anesthesia by gas inhalation (1% isofluorane/oxygen) before scanning in a microPET Focus 120 (Concorde Microsystems) at various times from 3 to 64 hours post-injection (p.i.). The *in vivo* stability of ^{124}I-hu3F8-C825 was confirmed by serial blood sampling via the tail-vein and silica-gel–impregnated glass-fiber thin layer chromatography (TLC) paper (Pall Corporation) with 10% trichloroacetic acid (Sigma-Aldrich) elution; ≥90.3% of ^{124}I-activity was protein associated at 64 hours p.i. Images were collected and processed as described previously, except with parameters for ^{124}I (19). Curve fitting of manually drawn two-dimensional region of interest (ROI) data (as ROI_{MAX}; %ID/g) was performed with Prism 6.0 (GraphPad) software. Select groups of mice were sacrificed immediately following PET for assay of radioactivity in select organs by gamma scintillation counting. For scintigraphy studies, mice previously injected with optimum doses of hu3F8-C825 and CA (1.75 mg of hu3F8-C825 and 250 μg (14% (w/w)) of 61 (Y)-DOTA-Bn/dextran, respectively), and 11.1 to 11.5 MBq of ^{177}Lu-DOTA-Bn were placed under anesthesia by gas inhalation before scanning in a nanoSPECT (BioScan) at 4 and 20 hours p.i. for 30 minutes (~10^5 counts/image) using a low-energy high-resolution collimator and a window set at 208 keV. Images were reconstructed to a 256 × 256 matrix using BioScan HiSPECT software and uploaded into ASIPro VM for analysis. The whole-body activity (WBA) for each mouse was determined by assay in the dose calibrator immediately following image acquisition.

Absorbed dose calculations

Two separate biodistribution studies were conducted to account for the different batch of CA compared with what was used during the CA dose optimization efforts [the (Y)-DOTA-Bn/dextran substitution ratio was 161 (Y)-DOTA-Bn/dextran during the CA dose optimization, and 61 (Y)-DOTA-Bn/dextran during the following experiments]. During the first set of experiments, groups of GD2(+)-NB IMR-32-Luc tumor-bearing mice ($n = 3$–4) were given 1.75 mg of hu3F8-C825, CA (125 μg; 7% (w/w) of 61 (Y)-DOTA-Bn/dextran), and 5.1 to 5.7 MBq (30–33 pmoles) of ^{177}Lu-DOTA-Bn, and sacrificed at 1, 3, 24, 96, 168, and 336 hours p.i. for biodistribution in normal tissue and tumor. The study was repeated a second time with a higher dose of CA (250 μg; 14% (w/w) of 61 (Y)-DOTA-Bn/dextran), with groups of mice ($n = 2$–5) sacrificed at 2, 24, 120, and 216 hours p.i. For each experiment, the nondecay-corrected time–activity concentration data

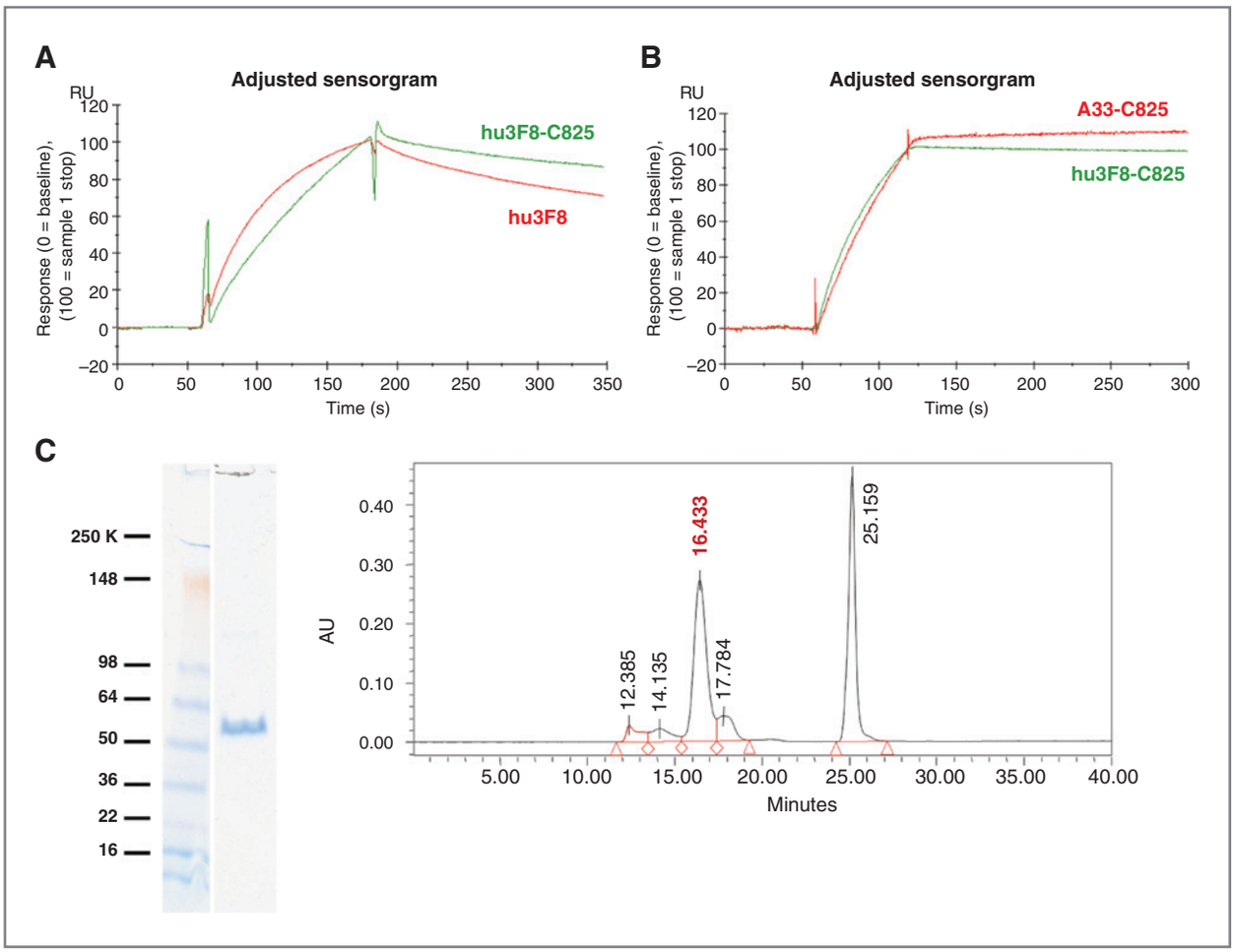

Figure 1. *In vitro* evaluation of hu3F8-C825 affinity and purity. Biacore sensorgrams of antibodies binding to GD2 (A), and to BSA-(Y)-DOTA-Bn (B). C, biochemical purity of hu3F8-C825; reduced SDS–PAGE (left) and SE-HPLC chromatogram (UV 280 nm) at right. The major peak (16.433 minutes) in SE-HPLC is the fully paired BsAb with an approximate MW of 210 kDa; 25.159 minutes is the salt buffer peak.

were fitted using Excel to a 1-component, a 2-component, or a more complex exponential function as appropriate, and analytically integrated to yield the cumulated activity concentration per unit administered activity (MBq h/g/MBq). The ^{177}Lu equilibrium dose constant for nonpenetrating radiations (8.49 gm cGy/MBq h) was used to estimate the tumor-to-tumor and select organ-to-organ self absorbed doses, assuming complete local absorption of the ^{177}Lu β rays only and ignoring the γ-ray and non–self-dose contributions. The biological clearance of activity (corrected for ^{177}Lu decay) from tumor and various tissues was determined by fitting the time–activity data to exponential functions using Prism 6.0 (GraphPad) software.

Therapy study

Mice bearing established GD2(+)-NB IMR-32-Luc subcutaneous tumors (tumor volume, 240 ± 160 mm^3) were randomized into two groups of 5 mice per group. One group was treated with three successive cycles of 1.75 mg of hu3F8-C825 (8.75 nmoles), 250 μg of CA (14% (w/w) of 61 (Y)-DOTA-Bn/dextran), and 11.1 MBq of ^{177}Lu-DOTA-Bn (∼60 pmoles). A time interval of 68 hours was allowed between each treatment cycle. The second group of mice received no treatment. This fractionated approach was used to allow for more efficient delivery of the dose compared with administration of a single cycle of hu3F8-C825, CA, and 33.3 MBq based on modeling estimates (see Supplementary Fig. S1). All mice were weighed and the tumor burden was assessed by caliper measurement every 3 to 4 days. In addition, luciferase imaging was conducted on the treated group using the Xenogen *In Vivo* Imaging System Spectrum (Caliper Lifesciences) at day −4 and 12 days after treatment to examine viable tumor cells at the xenograft site. Briefly, mice were anesthetized by gas inhalation (1% isofluorane/oxygen) and injected intraperitonially with 0.2 mL solution of D-luciferin [prepared by dissolving 75 mg of D-luciferin potassium salt (Gold Biotechnology) in 5 mL of PBS, then stored in aliquots at

−20°C]. Luciferase images were collected 4 to 5 minutes p.i. using the following parameters: A 60-second exposure time, medium binning, and an 8 f per stop. Luciferase image analysis was performed using Living Image 3.0 (Caliper LifeSciences). Mice were sacrificed if the tumor was >1.0 cm^3 or lost >20% of body mass during the course of the study. The treated mice were sacrificed after 28 days after treatment for evaluation of acute toxicity by conducting hematology, clinical chemistry, and necropsy (all by the Laboratory of Comparative Pathology, Memorial Sloan Kettering Cancer Center).

Statistical analysis

Differences in tissue uptake between cohorts were statistically analyzed with the Student *t* test for paired data. Two-sided significance levels were calculated and a *P* value of <0.05 was considered statistically significant.

Results

In vitro assessment of BsAb functionality and biochemical purity

For antigen GD2, hu3F8-C825 had a k_{on} of 5.96×10^4 1/(mol/L)/s, a k_{off} of 1.68×10^{-3} per second, and overall K_D of 28.2 nmol/L; comparable with parental hu3F8 (k_{on} of 1.79×10^5 1/(mol/L)/s, k_{off} of 2.91×10^{-3} per second, and overall K_D of 16.3 nmol/L; Fig. 1A). For antigen BSA-(Y)-DOTA-Bn, hu3F8-C825 had a k_{on} of 2.95×10^4 1/(mol/L)/s, a k_{off} of 2.84×10^{-4} per second, and overall K_D of 9.63 nmol/L; comparable with A33-C825 (k_{on} of 2.73×10^4 1/(mol/L)/s, k_{off} of 9.82×10^{-5} per second, and overall K_D of 3.60 nmol/L; Fig. 1B). In summary, hu3F8-C825 retained high binding affinity to both GD2 and BSA-(Y)-DOTA-Bn, especially the very slow k_{off} comparable with its parental hu3F8, a parameter considered critical for therapeutic efficacy.

Biochemical purity analysis of hu3F8-C825 by SDS–PAGE and SE-HPLC is shown in Fig. 1C. Under reducing SDS–PAGE conditions, hu3F8-C825 gave rise to two bands at around 50 kDa, because the C825–scFv fusion to hu3F8 light chain increased the MW to approximately 50 kDa. SE-HPLC showed a major peak (70% by UV analysis) with an approximate MW of 210 kDa, as well as some minor peaks assumed to be aggregates and lower MW protein fragments, removable by gel filtration. Isoelectric focusing (IEF) analysis showed a single band at around pH 9.5 (data not shown). The BsAb remained stable by SDS–PAGE, SE-HPLC, and BIACORE after multiple freeze and thaw cycles (data not shown).

In vivo pharmacokinetics and biodistribution of radiolabeled hu3F8-C825 in nude mice bearing subcutaneous GD2(+)-NB

PET-derived tumor and blood activity curves for ^{124}I-hu3F8-C825 up to 64 hours p.i. are shown in Supplementary Fig. S2. The blood clearance of hu3F8-C825 was biphasic [$t_{1/2}$ α of 2.8 hours and $t_{1/2}$ β of 14.6 hours ($R^2 = 0.989$)], with longer half-lives compared with 5F11-scFv-SA ($t_{1/2}$ α, 0.2 hours; $t_{1/2}$ β, 9.3 hours), but shorter than those previously reported for 3F8 IgG (e.g., 33 hours for ^{111}In-3F8; ref. 20). Tumor uptake of ^{124}I-hu3F8-C825 increased to approximately 5%ID/g within 12 hours p.i. and remained consistent for the following 24 hours p.i. The peak activity was 5.7%ID/g at approximately 22 hours p.i. From 36 to 64 hours p.i., the activity decreased gradually to a minimum of 3.3%ID/g. On the basis of these data, a time interval of 24 hours was allowed between the hu3F8-C825 and CA injections for PRIT. Immediately following PET scanning at 48 hours p.i., select tissues were harvested for biodistribution assay *ex vivo*. Activities in GD2(+)-NB tumor and blood matched those derived using PET, and low uptake and retention in normal tissue (e.g., <1.5%ID/g for spleen and kidney) was observed compared with tumor (~2.5%ID/g; Supplementary Fig. S3).

Biodistribution studies of PRIT with hu3F8-C825, CA, and ^{177}Lu-DOTA-Bn aimed at GD2(+)-NB

The optimum hu3F8-C825 and CA doses for PRIT were determined using a series of ^{177}Lu-DOTA-Bn

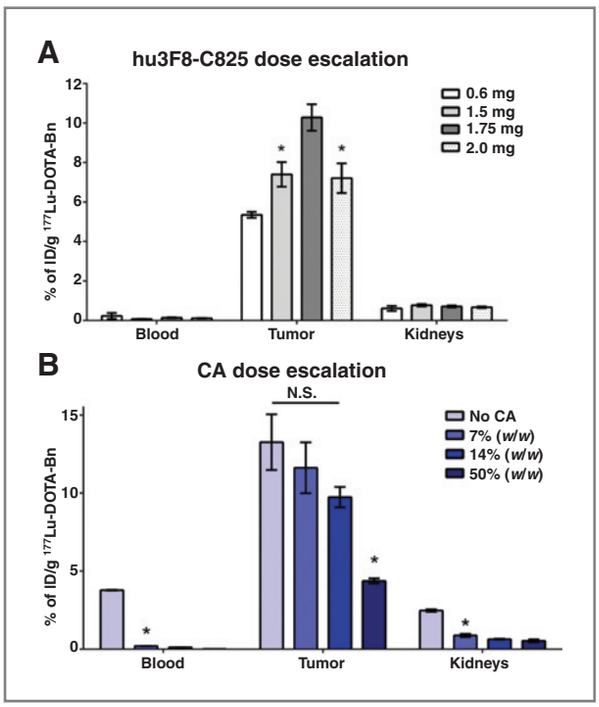

Figure 2. Biodistribution studies to optimize PRIT hu3F8-C825 and CA doses. A, optimization of hu3F8-C825 dose. Groups of GD2(+)-NB tumor-bearing mice were given 0.6 to 2.0 mg of hu3F8-C825, followed with approximately 12.5% (w/w) to hu3F8-C825 dose of 161 (Y)-DOTA-Bn/dextran and equal doses of ^{177}Lu-DOTA-Bn (5.6 MBq; ~30 pmoles). Mice were sacrificed 24 hours p.i. of ^{177}Lu-DOTA-Bn for biodistribution analysis; *, $P < 0.05$. B, optimization of CA dose. Groups of GD2(+)-NB tumor-bearing mice were given 1.75 mg of hu3F8-C825, followed with 0 to 0.875 mg (0%–50% (w/w)) of 161 (Y)-DOTA-Bn/dextran, and equal doses of ^{177}Lu-DOTA-Bn (5.6 MBq; ~30 pmoles). Mice were sacrificed 24 hours p.i. of ^{177}Lu-DOTA-Bn for biodistribution analysis; N.S., not significant; *, $P < 0.05$.

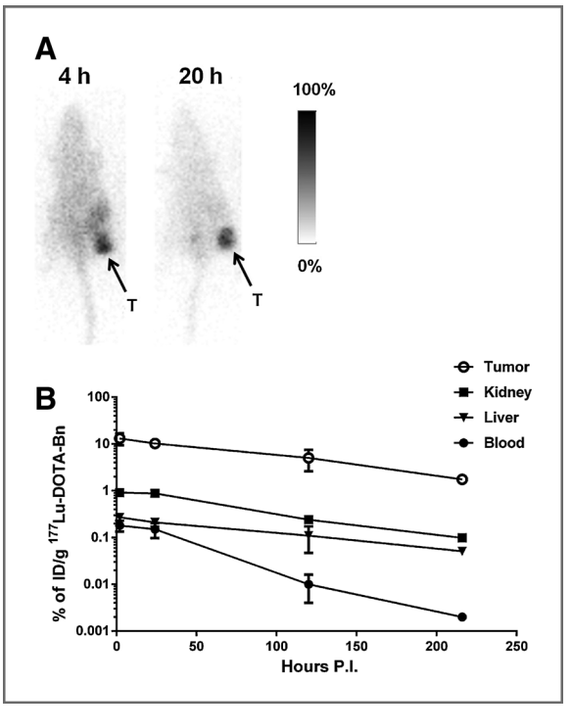

Figure 3. A, scintigraphic studies of PRIT, including optimum doses of hu3F8-C825 and CA. GD2(+)-NB tumor-bearing mice were injected with 1.75 mg of hu3F8-C825, followed 20 hours later with CA [250 μg; 14% (w/w) of 61 (Y)-DOTA-Bn/dextran], and ^{177}Lu-DOTA-Bn (11.2 MBq; ∼60 pmoles) after an additional 4 hours. Mice were imaged at 4 and 20 hours p.i. of ^{177}Lu-DOTA-Bn. Representative planar images are shown; T, tumor. The effective WBA was 2.0 MBq (17.9% of initial activity) and 0.85 MBq (7.6% of initial activity) at 4 and 20 hours p.i., respectively. B, ^{177}Lu-activity (as %ID/g, average ± SEM; corrected for nuclide decay) biodistribution curves up to 216 hours p.i. for tumor and select critical organs following PRIT with 5.6 MBq (∼30 pmoles) of ^{177}Lu-DOTA-Bn in nude mice carrying subcutaneous GD2(+)-NB xenografts.

biodistribution experiments in groups of mice bearing subcutaneous GD2(+)-NB IMR-32-Luc tumors. First, hu3F8-C825 was tested at four different dose levels: 0.6 (∼3 nmoles), 1.5, 1.75, and 2 mg per mouse (all $n = 5$ except for the cohort given 0.6 mg, which was $n = 2$). After injection with hu3F8-C825, all groups received 24 hours later, a proportional dose of CA [∼12.5% (w/w) of the antibody mass (12.7 ± 3.9%; mean ± SD) of CA (161 (Y)-DOTA-Bn/dextran)] and finally, after 4 hours, equal doses of ^{177}Lu-DOTA-Bn (5.6 MBq; 30 pmoles) were given. Shown in Fig. 2A, we observed that PRIT with 1.75 mg of hu3F8-C825 resulted in the greatest ^{177}Lu-DOTA-Bn uptake in tumor after 24 hours (10.3%ID/g; e.g., compared with 1.5 or 2.0 mg: 7.4 and 7.2%ID/g, respectively; $P < 0.05$). Next, the CA dose was titrated (0–0.875 mg; 0%–50% (w/w) of 161 (Y)-DOTA-Bn/dextran; $n = 2$ animals for vehicle cohort, and $n = 3$ for all CA cohorts) following injection with 1.75 mg (i.e., the optimum dose) of hu3F8-C825. Shown in Fig. 2B, all CA doses were shown to be effective at improving T/NT ratios (e.g., for blood and kidney) compared with vehicle by significantly reducing the uptake of ^{177}Lu-DOTA-Bn in normal tissues. Tumor uptake of ^{177}Lu-DOTA-Bn was attenuated at high doses of CA (e.g., 50% (w/w) CA; $P < 0.05$ compared with vehicle). The reduction in tumor activity was presumably due to the CA (or associated metabolites) occupying hu3F8-C825 at the tumor, causing the displacement or the blocking of ^{177}Lu-DOTA-Bn uptake by the BsAb. Representative planar SPECT images of a mouse given optimum hu3F8-C825 and CA doses and 11.1 MBq (∼60 pmoles) of ^{177}Lu-DOTA-Bn at 4 and 20 hours p.i. are shown in Fig. 3A.

The GD2 antigen specificity of hu3F8-C825, as well as the tumor uptake of ^{177}Lu-DOTA-Bn without PRIT, was evaluated in tumor-bearing mice. Studies included: (1) injection of ^{177}Lu-DOTA-Bn alone into groups of mice

Table 1. Comparison of biodistribution of ^{177}Lu-DOTA-Bn 24 hours p.i. alone or in combination with PRIT with hu3F8-C825 and CA

	PRIT with hu3F8-C825 and CA ($n = 5$)	^{177}Lu-DOTA-Bn only ($n = 2$)
Tissues		
Blood	0.14 ± 0.02	0.002 ± 0.00
Heart	0.09 ± 0.02	0.01 ± 0.00
Lungs	0.31 ± 0.04	0.02 ± 0.00
Liver	0.20 ± 0.02	0.06 ± 0.02
Spleen	0.48 ± 0.11	0.03 ± 0.00
Stomach	0.04 ± 0.01	0.17 ± 0.15
Small intestine	0.07 ± 0.01	0.03 ± 0.01
Large intestine	0.15 ± 0.03	0.55 ± 0.23
Kidneys	0.71 ± 0.05	0.78 ± 0.01
Muscle	0.09 ± 0.02	0.01 ± 0.00
Bone	0.09 ± 0.01	0.01 ± 0.00
Tumor	10.28 ± 0.67	0.04 ± 0.00
Tumor-to-tissue ratios		
Blood	73.5 ± 10.5	24.9 ± 0.3
Heart	114.8 ± 26.8	3.3 ± 0.3
Lungs	33.2 ± 5.0	2.1 ± 0.1
Liver	52.2 ± 6.6	0.7 ± 0.1
Spleen	21.5 ± 5.0	1.5 ± 0.1
Stomach	250.4 ± 55.0	0.2 ± 0.2
Small intestine	151.9 ± 31.5	1.3 ± 0.3
Large intestine	66.9 ± 12.2	0.1 ± 0.0
Kidneys	14.5 ± 1.5	0.1 ± 0.0
Muscle	118.5 ± 22.6	3.9 ± 1.5
Bone	117.9 ± 17.5	5.2 ± 1.0

NOTE: For PRIT with hu3F8-C825, nude mice bearing subcutaneous GD2(+)-NB tumors were given 1.75-mg hu3F8-C825, CA (250 μg; 14% (w/w) 161 (Y)-DOTA-Bn/dextran), and 5.6 MBq (∼30 pmoles) ^{177}Lu-DOTA-Bn. For ^{177}Lu-DOTA-Bn only, a separate group of nude mice bearing subcutaneous GD2(+)-NB tumors was injected with 5.6 MBq (∼30 pmoles) ^{177}Lu-DOTA-Bn. Results are given as mean %ID/g ± SEM.

Table 2. Absorbed doses for tumor and select normal tissue in mice carrying subcutaneous GD2(+)-NB tumors for PRIT, including two different doses of CA

Tissues	7% (w/w) CA cGy/MBq	Therapeutic index	14% (w/w) CA cGy/MBq	Therapeutic index
Blood	2.1	33	0.6	142
Tumor	70.0		84.9	
Heart	2.1	34	0.7	121
Lung	5.2	13	3.5	24
Liver	6.1	11	2.1	40
Spleen	10.4	7	2.0	42
Stomach	0.8	84	0.9	94
Small intestine	1.2	56	0.8	106
Large intestine	3.5	20	2.1	40
Kidneys	11.5	6	3.7	23
Muscle	1.8	39	1.0	85
Bone	1.2	60	0.7	121

NOTE: For each target region, the absorbed dose was calculated as the product of the ^{177}Lu equilibrium dose constant for nonpenetrating radiations (i.e., β-rays) and the target region's ^{177}Lu cumulated activity, assuming complete local absorption of the ^{177}Lu β-rays and ignoring the γ-ray and non–self-dose contributions.

bearing GD2(+)-NB IMR-32-Luc tumors (2), PRIT of GD2(−) BT474 tumors with hu3F8-C825, and (3) PRIT of GD2(+)-NB IMR-32-Luc with an irrelevant IgG-scFv (A33-C825). These data are shown in Table 1 and Supplementary Tables S1 and S2. Shown in Table 1, without PRIT with hu3F8-C825 and CA (i.e., injection of ^{177}Lu-DOTA-Bn alone), ^{177}Lu-DOTA-Bn exhibited rapid clearance and very low whole-body retention in mice bearing GD2(+)-NB tumors, comparable with previous biodistribution studies in mice (9). PRIT of GD2(−) BT474 tumors with hu3F8-C825 and ^{177}Lu-DOTA-Bn showed minimal uptake of ^{177}Lu-DOTA-Bn in tumor, suggesting that hu3F8-C825 failed to prelocalize appreciably in antigen-negative tumor (Supplementary Table S1). A parallel study comparing PRIT in mice bearing GD2(+)-NB with either an irrelevant IgG-scFv or hu3F8-C825 showed reduced ^{177}Lu-DOTA-Bn at the tumor (2.25 and 8.21%ID/g, respectively) as well as T/NT ratios <1 for normal tissues for the irrelevant IgG-scFv, suggesting specific uptake for hu3F8-C825 (Supplementary Table S2).

Absorbed dose estimates

For the first set of experiments in which PRIT was carried out with the lower CA dose[125 μg; 7% (w/w) of 61 (Y)-DOTA-Bn/dextran], the estimated absorbed doses of ^{177}Lu-DOTA-Bn (as cGy/MBq) for blood, tumor, liver, spleen, and kidney were 2.1, 70.0, 6.1, 10.4, and 11.5, respectively (Table 2). When the study was repeated using the higher dose of CA [250 μg; 14% (w/w) of 61 (Y)-DOTA-Bn/dextran], the estimated absorbed doses of ^{177}Lu-DOTA-Bn for blood, tumor, liver, spleen, and kidney were 0.6, 84.9, 2.1, 2.0, and 3.7, respectively (also in Table 2). The estimated dose to kidney was highest among normal tissues, thus presumed to be dose limiting. Decay-corrected time–activity curves for tumor and various tissues up to approximately 220 hours p.i. obtained with the higher CA dose are shown in Fig. 3B. Average tumor uptake was 10.2%ID/g at 24 hours p.i. and cleared with a $t_{1/2}$ of 80.3 hours ($R^2 = 0.994$). Peak kidney, liver, and blood uptake was observed at 2 hours p.i. (0.91, 0.27, and 0.18%ID/g, respectively). Activity from kidney and liver cleared at a slower rate than blood (kidney $t_{1/2}$: 68.0 hours, $R^2 = 0.968$; liver $t_{1/2}$: 77.4 hours, $R^2 = 0.994$; blood $t_{1/2}$: 41.0 hours, $R^2 = 0.973$), suggesting prolonged retention and/or nonspecific uptake of ^{177}Lu-DOTA-Bn (or hu3F8-C825-^{177}Lu-DOTA-Bn complex) in those tissues.

Therapy study

A description of the treatment schedule, which included three successive PRIT injection cycles (total ^{177}Lu dose: 33.3 MBq), is provided in Fig. 4A. The tumor response curves for treated and nontreated groups are shown in Fig. 4B. For treated mice, tumors started to respond substantially (i.e., >50% reduction) after the second injection cycle, and complete tumor ablation was observed in 2 of 5 mice within 10 days following the last injection of ^{177}Lu-DOTA-Bn. All nontreated mice had uncontrolled tumor growth to beyond 1.0-cm^3 size requiring euthanasia within 12 days (or ∼40 days following tumor inoculation; shown in Fig. 4C). Luciferase imaging of treated mice at day −4 showed signals at the tumor site ranging from approximately 10^4 to 10^6 × photons/s/cm^2/sr, whereas at 12 days after treatment showed no signal at the tumor site (data not shown). The treated mice cohort was sacrificed at 28 days after treatment for hematology, clinical chemistry, and necropsy analyses to evaluate gross and histologic toxicities to normal tissues, as well

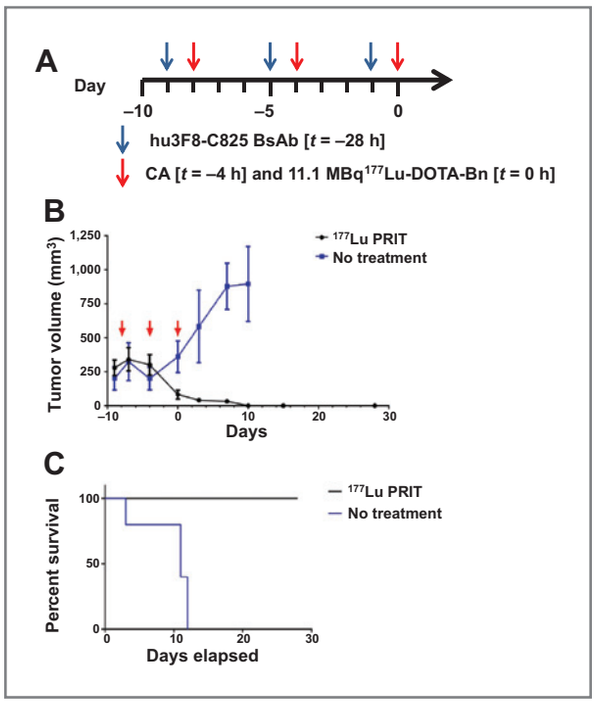

Figure 4. A, PRIT treatment schedule. Groups of GD2(+)-NB tumor-bearing mice ($n = 5$) received either three successive cycles of 1.75 mg of hu3F8-C825, CA (250 μg; 14% (w/w) of 61 (Y)-DOTA-Bn/dextran), and approximately 11.1 MBq (~60 pmoles) of ^{177}Lu-DOTA-Bn, with 68 hours between each cycle, or no treatment. B, comparison of tumor volumes of either treated or nontreated groups of animals during treatment study, up to 28 days after therapy. C, survival curve for treated and nontreated groups of mice. Animals not treated with PRIT required sacrifice within 12 days due to excessive tumor size (>1.0 cm^3).

as obtain a histologic assessment of any residual tumor at the subcutaneous xenograft site. In 3 of 5 mice, too-small-to-measure residual masses at the site of the xenograft showed microscopically residual NB in 1 mouse, but only lipid laden macrophages in the other 2. During the course of the study, all mice maintained body mass (i.e., no changes greater than 20% between weighing intervals), and were in good visible health, suggesting low overall treatment toxicity (data not shown). Hematology showed no anemia (Supplementary Table S3) but polychromasia of red blood cells and increased reticulocyte counts in all mice (data not shown), suggesting a regenerative response. In addition, all treated animals showed total white blood cell counts and hemoglobin within normal ranges, but a slight decrease in platelets (Supplementary Table S3). Histologic analysis (data not shown) of bone marrow and spleen revealed myeloid hyperplasia (mild to moderate, subacute) in 3 of 5 mice. For kidney, 1 of 5 was normal, whereas in 3 of 5 mice the vessels were mildly ectatic, with rare cortical tubules lined by slightly plump epithelial cells with weakly basophilic cytoplasm, and in 1 mouse, a kidney showed an infarct of the cortex and medulla, with collapsed to mildly ectatic tubules in the area (data not shown). All serum chemistry values, including those indicating renal function, were within reference ranges (Supplementary Table S3).

Discussion

In this study, we evaluated PRIT of GD2(+)-NB using a novel BsAb containing sequences for an anti-GD2 mAb hu3F8 (8) and an anti-DOTA(metal) scFv (6). Using the optimum PRIT parameters determined during initial experiments, we showed that a treatment schedule consisting of three successive cycles (total ^{177}Lu-DOTA-Bn: 33.3 MBq), was sufficient to achieve complete tumor responses in 5 of 5 mice within 10 days after treatment, including tumor ablation in 4 of 5 animals, as well as no tumor recurrence and low overall toxicity up to 28 days after treatment. Complete tumor response after 12 days was also confirmed using luciferase measurements as a secondary endpoint, showing no viable cells at the xenograft site.

For PRIT at current optimized doses of hu3F8-C825 and CA and approximately 5.4 MBq of ^{177}Lu-DOTA-Bn, absorbed doses for tumor and kidney are approximately 85 and 3.7 cGy/MBq, respectively. To estimate doses delivered in our pilot study, we assumed that the dose estimates obtained with 5.4 MBq of ^{177}Lu-DOTA-Bn (~30 pmoles) would be valid for 11.1 MBq (~60 pmoles); hence, three cycles with 11.1 MBq ^{177}Lu/cycle (33.3 MBq total) would deliver estimated doses of approximately 3,400 cGy to the tumor (see Supplementary Fig. S1), <~120 cGy to kidney, and <20 cGy to blood. Although these parameters need to be optimized to reduce bystander radiation especially to liver and kidney, the lack of toxicities in our xenograft studies are encouraging. Our results agree with the prediction of Press and colleagues that, because of the superior TI of PRIT, administration of a ^{90}Y dose as high as twice the lethal dose using non-pretargeted RIT was possible with negligible toxicity (21).

The relatively high kidney exposure compared with other normal tissues is presumably due to capture of hapten by BsAb localized at the organ, because renal dose estimates for ^{177}Lu-DOTA-Bn alone are only 0.01 cGy/MBq (9). Nonetheless, this is a substantial improvement in TI seen for PRIT directed at GD2(+)-NB with 5F11-scFv-SA, which showed higher doses to both tumor and kidney (approximately 150 and 50 cGy/MBq, respectively), and a TI for kidney of approximately 3:1. These data are also promising compared with other PRIT strategies, including those with BsAb against tumor antigens and histamine–succinyl–glycine (HSG) hapten, pioneered by Sharkey and colleagues (22). For example, they showed in preclinical mouse models of CEA-expressing tumors, absorbed radiation dose estimates for PRIT with anti-CEA/HSG BsAb and ^{177}Lu-hapten (~23 MBq) were 16.9 Gy for a 6-mm subcutaneous tumor and 2.3 Gy for kidney, corresponding to approximately 73 and 10 cGy/MBq, respectively (TI for kidney >7:1; ref. 23).

GD2(+)-NB IMR-32 is not a particularly radioresistant human NB cell line (24), and we anticipate that some

tumors may require higher doses >3,400 Gy to demonstrate tumor response. Our radiation exposure benchmarks for curative PRIT of GD2(+)-NB (i.e., for ablation without recurrence) are based on prior experience to be ≥4,200 cGy in tumor (18) at the expense of a maximum kidney exposure of approximately 2,500 cGy (25). To achieve this tumor dose of 4,200 cGy, we estimate a single-cycle treatment with the higher CA dose and a ^{177}Lu-DOTA-Bn dose of approximately 50 MBq is required, exposing the blood and kidney to approximately 30 and 185 cGy, respectively (Table 2). In addition to conducting these studies, there are a number of different approaches that we intend to explore to improve the TI of this PRIT strategy, including (1) optimization of hu3F8-C825 tumor uptake and pharmacokinetics, and (2) optimization of the CA step. The relatively high hu3F8-C825 dose of 1.75 mg (8.75 nmoles) was found to be required to achieve high absolute tumor uptake, which is greater than previous PRIT studies directed at GD2(+)-NB (5.2 nmoles for 5F11-scFv-SA), most likely a function of bivalency of hu3F8-C825 versus tetravalency of 5F11-scFv-SA. This is likely a function of the antigen density ($0.6–2.0 \times 10^6$ molecules per cell) although improving tumor-targeting efficiency and *in vivo* stability of the BsAb may theoretically decrease the dose required to achieve saturation (26). One approach is to optimize the hu3F8-C825 affinity or half-life in circulation (27). Yazaki and colleagues suggested that despite serum stability of this IgG-scFv BsAb platform, the murine version of C825 resulted in accelerated clearance of the BsAb by the mononuclear phagocyte system *in vivo* (28). The Wittrup group has developed a humanized version of C825 that could avoid this clearance issue, besides further reducing the immunogenicity of these constructs in humans (28). Second, when hu3F8 was humanized, its affinity for GD2 (especially k_{off}) was slightly reduced (8). We have since used an affinity maturation procedure by yeast surface display (29) in which affinity of hu3F8 to GD2 was increased by 10- to 20-fold (data not shown). Finally, although the affinity of C825 was already matured to the pmol/L range (5), further improvement should be possible with an "infinite" affinity approach (30).

Improvement of the clearance step may also enhance tumor uptake of ^{177}Lu-DOTA-Bn, as well as the tumor-to-normal tissue ratios. The tumor-to-blood ratio at 24 hours p.i. was approximately 75:1 with dextran-based CA during our PRIT studies, but this is significantly less than that for PRIT with 5F11-scFv-SA and a biotinylated *N*-acetylgalactosamine-dendrimer CA, which showed tumor-to-blood ratios of approximately 450:1 as early as 30 hours p.i. (1). This could be attributed to the million-fold difference in affinity between streptavidin–biotin [$>10^{15}$ 1/(mol/L)] compared with C825-DOTA [$>10^9$ 1/(mol/L)], and the homotetrameric structure of streptavidin and 5F11-scFv-SA *in vivo* compared with bivalent binding for C825. As an alternative CA to dextran-(Y)-DOTA-Bn, a DOTA–hapten–*N*-acetylgalactosamine-dendrimer CA could promote clearance via Ashwell receptors present in the liver and enable excretion via the hepatobiliary route. In addition, the interval between administration of CA and ^{177}Lu-DOTA-Bn could be optimized to account for reticuloendothelial metabolism of CA–hu3F8–C825 complexes and potentially reduce associated metabolites in circulation.

Future studies will also include optimization of hapten dose and formulation, PRIT using ^{177}Lu-DOTA-Bn or DOTA-Bn radiolabeled with PET nuclides (e.g., ^{86}Y or ^{68}Ga) for imaging-guided dosimetry and therapy planning, as well additional treatment studies to further refine dose estimates to produce long-term cures in radioresistant GD2(+)-NB and possibly other GD2(+) tumors, and identify chronic toxicities especially if repeated cycles are to be given.

Conclusion

In this report, we show that PRIT using hu3F8 and C825 is a viable alternative to streptavidin-based therapies, overcoming the major limitation of renal uptake. Hu3F8 has low immunogenicity in human trials (clinicaltrials.gov NCT01419834, NCT01757626, and NCT01662804), and with the introduction of the humanized version of C825, the immunogenicity issue might be finally overcome to facilitate the clinical development of anti-GD2 MST.

Disclosure of Potential Conflicts of Interest

N.-K. Cheung has ownership interest (including patents) in hu3F8. No potential conflicts of interest were disclosed by the other authors.

Authors' Contributions

Conception and design: S.M. Cheal, H. Xu, P.B. Zanzonico, S.M. Larson, N.-K. Cheung
Development of methodology: S.M. Cheal, H. Xu, S.M. Larson, N.-K. Cheung
Acquisition of data (provided animals, acquired and managed patients, provided facilities, etc.): S.M. Cheal, H. Xu, H.-F. Guo, S.M. Larson, N.-K. Cheung
Analysis and interpretation of data (e.g., statistical analysis, biostatistics, computational analysis): S.M. Cheal, H. Xu, P.B. Zanzonico, S.M. Larson, N.-K. Cheung
Writing, review, and/or revision of the manuscript: S.M. Cheal, H. Xu, P.B. Zanzonico, S.M. Larson, N.-K. Cheung
Administrative, technical, or material support (i.e., reporting or organizing data, constructing databases): H.-F. Guo, S.M. Larson, N.-K. Cheung
Study supervision: S.M. Larson, N.-K. Cheung
Other: S.M. Cheal is a postdoctoral research fellow in the laboratory of S.M. Larson

Acknowledgments

The authors thank Dr. Dane Wittrup and his laboratory at Massachusetts Institute of Technology, Cambridge, MA for their generosity and expert advice. The authors also thank Dr. Vladimir Ponomarev for kindly providing the SFG-GFLuc vector. The authors thank Blesida Punzalan, Michael Doran, Sandhya Chalasani, Shoaib Fareedy, and Valerie Longo for their excellent technical assistance with the animal experiments.

Grant Support

This study was supported in part by the following: The Center for Targeted Radioimmunotherapy and Theranostics, Ludwig Center for Cancer Immunotherapy, Memorial Sloan Kettering Cancer Center (MSK; to S.M. Larson), a training grant from the NIH (R25-CA096945; principal investigator H. Hricak; research and salary support to S.M. Cheal), William H. Goodwin and Alice Goodwin and the Commonwealth Foundation for Cancer Research and The Experimental Therapeutics Center of MSK (to N.-K. Cheung), Kids Walk for Kids with Cancer NYC (to N.-K. Cheung),

and the Robert Steel Foundation (to N.-K. Cheung). S.M. Larson was also supported in part by P50-CA86438. Technical services provided by the MSK Small-Animal Imaging Core Facility were supported in part by NIH Grants R24-CA83084 (to H. Hricak), P30-CA08748 (to C. Thompson), and P50-CA92629 (to H. Scher). NIH Shared Instrumentation Grant No 1 S10 RR020892-01 (to S.M. Larson), NIH Shared Instrumentation Grant No 1 S10 RR028889-01 (to P.B. Zanzonico), and a Shared Resources Grant from the MSKCC Metastasis Research Center (to P.B. Zanzonico), which provided funding support for the purchase of the Focus 120 microPET, NanoSPECT/CT Plus, and Ivis Spectrum, respectively, are gratefully acknowledged.

The costs of publication of this article were defrayed in part by the payment of page charges. This article must therefore be hereby marked *advertisement* in accordance with 18 U.S.C. Section 1734 solely to indicate this fact.

Received October 30, 2013; revised March 31, 2014; accepted April 19, 2014; published OnlineFirst June 18, 2014.

References

1. Cheung NKV, Modak S, Lin YK, Guo HF, Zanzonico P, Chung J, et al. Single-chain Fv-streptavidin substantially improved therapeutic index in multistep targeting directed at disialoganglioside GD2. J Nucl Med 2004;45:867–77.
2. Sharkey RM, Goldenberg DM. Cancer radioimmunotherapy. Immunotherapy 2011;3:349–70.
3. Reardan DT, Meares CF, Goodwin DA, McTigue M, David GS, Stone MR, et al. Antibodies against metal chelates. Nature 1985;316:265–8.
4. Goodwin DA, Meares CF, Watanabe N, McTigue M, Chaovapong W, Ransone CM, et al. Pharmacokinetics of pretargeted monoclonal antibody 2D12.5 and 88Y-Janus-2-(p-nitrobenzyl)-1,4,7,10-tetraazacyclododecanetetraacetic acid (DOTA) in BALB/c mice with KHJJ mouse adenocarcinoma: a model for 90Y radioimmunotherapy. Cancer Res 1994;54:5937–46.
5. Orcutt KD, Slusarczyk AL, Cieslewicz M, Ruiz-Yi B, Bhushan KR, Frangioni JV, et al. Engineering an antibody with picomolar affinity to DOTA chelates of multiple radionuclides for pretargeted radioimmunotherapy and imaging. Nucl Med Biol 2011;38:223–33.
6. Orcutt KD, Ackerman ME, Cieslewicz M, Quiroz E, Slusarczyk AL, Frangioni JV, et al. A modular IgG-scFv bispecific antibody topology. Protein Eng Des Sel 2010;23:221–8.
7. Orcutt KD, Rhoden JJ, Ruiz-Yi B, Frangioni JV, Wittrup KD. Effect of small-molecule–binding affinity on tumor uptake *in vivo*: a systematic study using a pretargeted bispecific antibody. Mol Cancer Ther 2012;11:1365–72.
8. Cheung NK, Guo H, Hu J, Tassev DV, Cheung IY. Humanizing murine IgG3 anti-GD2 antibody m3F8 substantially improves antibody-dependent cell-mediated cytotoxicity while retaining targeting *in vivo*. Oncoimmunology 2012;1:477–86.
9. Orcutt KD, Nasr KA, Whitehead DG, Frangioni JV, Wittrup KD. Biodistribution and clearance of small-molecule hapten chelates for pretargeted radioimmunotherapy. Mol Imaging Biol 2011;13:215–21.
10. Battula VL, Shi Y, Evans KW, Wang RY, Spaeth EL, Jacamo RO, et al. Ganglioside GD2 identifies breast cancer stem cells and promotes tumorigenesis. J Clin Invest 2012;122:2066–78.
11. Ponomarev V, Doubrovin M, Serganova I, Vider J, Shavrin A, Beresten T, et al. A novel triple-modality reporter gene for whole-body fluorescent, bioluminescent, and nuclear noninvasive imaging. Eur J Nucl Med Mol Imaging 2004;31:740–51.
12. Corneillie TM, Whetstone PA, Fisher AJ, Meares CF. A rare earth-DOTA-binding antibody: probe properties and binding affinity across the lanthanide series. J Am Chem Soc 2003;125:3436–7.
13. Hermanson GT. Bioconjugate techniques. 2nd ed. London: Academic Press; 2008.
14. Hu J, Huang X, Ling CC, Bundle DR, Cheung NK. Reducing epitope spread during affinity maturation of an anti-ganglioside GD2 antibody. J Immunol 2009;183:5748–55.
15. Harlow E, Lane D. Using antibodies: a laboratory manual. Cold Spring Harbor, NY: Cold Spring Harbor Laboratory Press; 1999.
16. Salacinski PR, McLean C, Sykes JE, Clement-Jones VV, Lowry PJ. Iodination of proteins, glycoproteins, and peptides using a solid-phase oxidizing agent, 1,3,4,6-tetrachloro-3 alpha,6 alpha-diphenyl glycoluril (Iodogen). Anal Biochem 1981;117:136–46.
17. Miederer M, McDevitt MR, Sgouros G, Kramer K, Cheung NK, Scheinberg DA. Pharmacokinetics, dosimetry, and toxicity of the targetable atomic generator, 225Ac-HuM195, in nonhuman primates. J Nucl Med 2004;45:129–37.
18. Cheung NK, Landmeier B, Neely J, Nelson AD, Abramowsky C, Ellery S, et al. Complete tumor ablation with iodine 131-radiolabeled disialoganglioside GD2-specific monoclonal antibody against human neuroblastoma xenografted in nude mice. J Natl Cancer Inst 1986;77:739–45.
19. Holland JP, Divilov V, Bander NH, Smith-Jones PM, Larson SM, Lewis JS. 89Zr-DFO-J591 for immunoPET of prostate-specific membrane antigen expression *in vivo*. J Nucl Med 2010;51:1293–300.
20. Ugur O, Kostakoglu L, Hui ET, Fisher DR, Garmestani K, Gansow OA, et al. Comparison of the targeting characteristics of various radioimmunoconjugates for radioimmunotherapy of neuroblastoma: dosimetry calculations incorporating cross-organ beta doses. Nucl Med Biol 1996;23:1–8.
21. Press OW, Corcoran M, Subbiah K, Hamlin DK, Wilbur DS, Johnson T, et al. A comparative evaluation of conventional and pretargeted radioimmunotherapy of CD20-expressing lymphoma xenografts. Blood 2001;98:2535–43.
22. Sharkey RM, Karacay H, Chang CH, McBride WJ, Horak ID, Goldenberg DM. Improved therapy of non-Hodgkin's lymphoma xenografts using radionuclides pretargeted with a new anti-CD20 bispecific antibody. Leukemia 2005;19:1064–9.
23. Frampas E, Maurel C, Remaud-Le Saec P, Mauxion T, Faivre-Chauvet A, Davodeau F, et al. Pretargeted radioimmunotherapy of colorectal cancer metastases: models and pharmacokinetics predict influence of the physical and radiochemical properties of the radionuclide. Eur J Nucl Med Mol Imaging 2011;38:2153–64.
24. Russell J, Wheldon TE, Stanton P. A radioresistant variant derived from a human neuroblastoma cell line is less prone to radiation-induced apoptosis. Cancer Res 1995;55:4915–21.
25. O'Donoghue J. Relevance of external beam dose–response relationships to kidney toxicity associated with radionuclide therapy. Cancer Biother Radiopharm 2004;19:378–87.
26. Liu G, Hnatowich DJ. A semiempirical model of tumor pretargeting. Bioconjug Chem 2008;19:2095–104.
27. Graff CP, Wittrup KD. Theoretical analysis of antibody targeting of tumor spheroids: importance of dosage for penetration, and affinity for retention. Cancer Res 2003;63:1288–96.
28. Yazaki PJ, Lee B, Channappa D, Cheung CW, Crow D, Chea J, et al. A series of anti-CEA/anti-DOTA bispecific antibody formats evaluated for pre-targeting: comparison of tumor uptake and blood clearance. Protein Eng Des Sel 2013;26:187–93.
29. Zhao Q, Feng Y, Zhu Z, Dimitrov DS. Human monoclonal antibody fragments binding to insulin-like growth factors I and II with picomolar affinity. Mol Cancer Ther 2011;10:1677–85.
30. Corneillie TM, Whetstone PA, Lee KC, Wong JP, Meares CF. Converting weak binders into infinite binders. Bioconjug Chem 2004;15:1389–91.